

Fully differential cross sections for Li^{2+} -impact ionization of $Li(2s)$ and $Li(2p)$

Omid Ghorbani¹, Ebrahim Ghanbari-Adivi^{1,*} and Marcelo Fabian Ciappina²

¹ *Department of Physics, Faculty of Sciences, University of Isfahan, Isfahan 81746-73441, Iran*

² *Institute of Physics of the ASCR, ELI-Beamlines, Na Slovance 2, 182 21 Prague, Czech Republic*

A semiclassical impact parameter version of the continuum distorted wave-Eikonal initial state theory is developed to study the differential ionization of Li atoms in collisions with Li^{2+} ions. Both post and prior forms of the transition amplitude are considered. The fully differential cross sections are calculated for the lithium targets in their ground and their first excited states and for the projectile ions at 16 MeV impact energy. The role of the internuclear interaction as well as the significance of the post-prior discrepancy in the ejected electron spectra are investigated. The obtained results for ejection of the electron into the azimuthal plane are compared with the recent measurements and with their corresponding values obtained using a fully quantum mechanical version of the theory. In most of the cases, the consistency of the present approach with the experimental and the quantum theoretical data is reasonable. However, for $2p$ -state ionization, in the cases where no experimental data exist, there is a considerable difference between the two theoretical approaches. This difference is questionable and further experiments are needed to judge which theory makes a more accurate description of the collision dynamics.

PACS numbers: 34.80.Dp

I. INTRODUCTION

The study of the electronic reactions due to the collision of electrons and heavy ions with atomic and molecular targets is one of the interesting topics in atomic and molecular physics that has attracted considerable attention for many years. Apart from the challenges that appear in both experimental and theoretical investigations of such phenomena, there exist some other reasons that highlight the importance of these processes. For example, these reactions play a predominant role in applied areas such as the design of fusion reactors, the study of heavy-particle radiation damage in human tissues and the application of hadron therapy. Also, in many scientific areas such as astrophysics and plasma physics, a detailed knowledge of the mechanisms of these processes is usually required [1, 2]. However, one of the main aspects of these phenomena is the fact that they provide an interesting probe of the few-body problem (FBP) in physics [3]. The Coulomb interaction which is responsible for these reactions is exactly known, while the Schrödinger equation governing the dynamics of such systems is not analytically solvable for more than two mutually interacting particles. Consequently, the validity of the various approximate theories which are developed to shed light on questions relevant to dynamics of the few-body Coulomb systems should be assessed by comparing their predictions with precise experimental data.

When an energetic bare ion impacts an atomic or a molecular target, there is a definite probability for occurrence of each of the basic processes such as electron capture and excitation or ionization of the target. Among these various processes, ionization in particular has received a great part of attention, because not only it is

the main mechanism leading to the energy loss of the swift ions in matter but also, it provides an ideal testing ground for the Coulomb FBP [4, 5]. This is especially true for the single ionization of the target for which there are three unbound particles in the final state [6]. More challenge to theoretical models for proving their accuracy comes from the measured fully differential cross sections (FDCSs), because the more differential cross sections, the more information that can be derived about the collision mechanism. In the case of electron impact, the kinematically complete experiments have provided a remarkable amount of the measured FDCSs to investigate the few-body aspects of the $(e, 2e)$ processes [7–11]. In such experiments, the complete momentum vectors of all the collision fragments are determined. For the case of ion impact, since both the scattering angles and the changes in the magnitude of the projectile momentum are very small, these experiments are much more challenging. It took a long time after the corresponding experiment for electron impact which the difficulties associated with the large projectile mass were circumvented by measuring the momentum vectors of the recoiling target ion and the ejected electron, using the novel method of the cold-target recoil-ion momentum spectroscopy (COLTRIMS) (also known as a reaction microscope (ReMi)) [3, 12, 13]. The scattered projectile momentum can then be deduced from the kinematic conservation laws. COLTRIMS is limited to gaseous targets of relatively small mass number. In order to overcome this limitation, the supersonic gas jet applied to produce the very cold target beam in a conventional reaction microscope was replaced by a magneto-optical trap (MOT) to innovate the MOTReMi method [14, 15]. This method improved the achievable recoil-ion momentum resolution considerably and extended the targets to heavy atoms or molecules which can be optically pumped.

Development of the above mentioned experimental

* ghanbari@phys.ui.ac.ir

techniques has renewed the interest in the theoretical study of the ion-impact ionization of the atomic and molecular targets. A number of the theoretical studies engaging these reactions have been done in framework of the time dependent close coupling (TDCC) [16], classical trajectory Monte Carlo (CTMC) [17, 18], continuum distorted wave-Eikonal initial state (CDW-EIS) [19, 20], coupled pseudostate (CP) [21, 22] and three-body distorted wave-Eikonal initial state (3DW-EIS) [23] theories.

Very recently, the measured FDCSs for 16 MeV Li^{2+} single ionization of the $2s$ ground and the $2p$ excited states of lithium has been reported and compared with the 3DW-EIS calculations [24]. The study of this reaction is of interest for several reasons. First, the radial nodal structure of the $2s$ and $2p$ wavefunctions as well as the angular distribution of the $2p$ wavefunction of the valence electron may lead to some structures in the FDCS. Second, in the lithium targets, the inner shell is both spatially and energetically far away from the valence shell which includes a single valence electron. So, it is expected that the electron-electron correlation plays a marginal role in the collision dynamics. Additionally, for this system the perturbation parameter (projectile charge to speed ratio) is much larger than that for a typical ($e, 2e$) reaction. This in combination with the more complex structure of the wavefunctions can lead to new features not seen previously. The reported data are for ejection into the azimuthal plane and the comparisons showed that the $2s$ and $2p$ cross sections exhibit different behaviors in some features. For example, for the $2p$ case, a double binary peak structure was theoretically predicted for some values of the projectile momentum transfer and the ejected electron energy, while such a structure is absent for some other values of these quantities. Using the 3DW-EIS method, it was shown that the double peak structure is associated to the kinematics of the reaction and to the angular part of the wavefunction. Although, the good overall agreement was found between the 3DW-EIS calculations and the experimental data, there exist some discrepancies which motivate further investigation of the process.

In this contribution, we apply the semiclassical CDW-EIS method [26, 27] to calculate the fully differential cross sections for single ionization of Li in collision with 16 MeV Li^{2+} projectile ions. The followed approach in fact provides an approximate solution to the Schrödinger equation governing the dynamics of the specified collisional breakup process which in turn is approximated to a three-body reaction with effective Coulomb interactions. The solution satisfies both the initial and final correct boundary conditions. In this treatment a classical straight-line trajectory is considered for the projectile, while the states of the involving particles are described quantum mechanically. For an impact energy of 16 MeV, assuming a classical straight-line trajectory for the projectile is not too far from reality. Also, as is mentioned above, the single optical active electron in

Li atoms is spatially far away from the spherically symmetric full inner shell closest to the nucleus. So, approximating the core interaction with the active electron and the projectile ion as the Coulomb interactions (with an effective charge) is not too rough. Indeed, in the present study, we use a linear combination of the hydrogenic wave functions, Roothaan-Hartree-Fock (RHF) wave functions [25], to make an analytical fit to the numerical Hartree-Fock (HF) wave functions. It is well known that the three-dimensional wave functions can be approximated as an expansion in terms of the hydrogenic wave functions as a complete set. These assumptions, may make the calculations easier, but it does not mean that such a complicated problem is reduced to a simple hydrogenic problem. The obtained results are discussed in comparison with experimental data and with the calculations of the full quantum mechanical version of the theory. Comparison shows that the mentioned assumptions give a reasonable estimate of the FDCSs.

Over the years, it has been shown that CDW-EIS theory is one of the most successful approaches to explain the dynamics of ion-atom collisional processes in the perturbative regime. We considered a number of assumptions to perform the CDW-EIS calculations easier and faster to do, and the reported results show that these assumptions do not significantly affect the accuracy of the calculations. Our further study on Li^{2+} - Li system using 3DW-EIS shows that if we use an analytical fit to the numerical HF wavefunction and employ a Coulomb potential to approximate the interaction with the passive electron, the obtained results will not change significantly in shape. These facts motivated us to use an analytical RHF wave function for the initial electronic state and use the Coulomb potentials to describe the interaction of the target core with the projectile and the active electron. This simplification reduces the computing time considerably. For example, for the $2p$ -state ionization and for each specified values of the ejected-electrons energy and the projectile momentum transfer, the 3DW-EIS calculations occupy 60 CPUs for nearly 45 hours, while with our present CDW-EIS approach the same results are obtained using only one CPU through several minutes.

The plan of the paper is as follows. Section II presents the impact parameter version of the CDW-EIS model to investigate a typical ion-impact ionization process. Section III is devoted to the results and the relevant discussions, and section IV includes the summary and concluding remarks. Atomic units ($e = m_e = \hbar = 1$) are used unless otherwise stated.

II. THEORY

The continuum distorted wave-Eikonal initial state (CDW-EIS) approach was firstly introduced by Crothers and his coworkers [26, 27] and applied as a successful method to treat a wide variety of collision systems [19, 20, 28–41], so only a brief outline will be given

here.

A number of simplifying assumptions is convenient in theoretical investigation of a typical ion-atom collision system. The assumptions which are used in the present model are as follows. (a) We use the frozen-core approximation in which one of the electrons of the target is considered as the active electron and the others are considered frozen in their initial states as the passive ones. The influence of the passive electrons is considered through the effective screening potential in the calculations. (b) In the semi-classical CDW-EIS model, the impact-parameter approximation is used. In this approximation, a straight-line trajectory is considered to describe the relative motion of the nuclei. Consequently, the inter-nuclear position vector is parameterized by the impact parameter $\boldsymbol{\rho}$ and the constant relative velocity \mathbf{v} as $\mathbf{R}(t) = \boldsymbol{\rho} + \mathbf{v}t$ with $\boldsymbol{\rho} \cdot \mathbf{v} = 0$. Hence, the closest distance between the heavy particles occurs at the time $t = 0$. (c) The RHF wavefunctions are employed to describe the state of the bound subsystem in the entrance channel [25]. (d) In the final channel, the potential interaction between the ionized electron and the residual target ion is approximated by an effective Coulomb potential. (e) the final continuum-state of the ionized electron in the field of the residual target ion is considered as a Coulomb wave.

By these assumptions and working in the framework of the independent-electron frozen-core model, the collision system can be reduced to a three-body system including a bare projectile ion P , with charge of Z_P and mass of M_P , the active electron e , and the target ion T with an effective charge of Z_T and mass of M_T . It is assumed that P impinges on $(T + e)$ with the initial wave vector \mathbf{K}_i . Over the course of the collision, P is scattered with the final momentum \mathbf{K}_f and e is ejected with wave vector \mathbf{k}_e . The full electronic Hamiltonian of these three-body system reads [29]

$$H_{el} = H_0 + V_P(|\mathbf{R} - \mathbf{r}|) + V_S(R), \quad (1)$$

in which \mathbf{r} is the position vector of the active electron with respect to T , H_0 is the Hamiltonian for the free target atom and $V_P(|\mathbf{R} - \mathbf{r}|)$ and $V_S(R)$ denote the P - e and P - T interactions. The effective nucleus charge is considered as $Z_{eff} = n_i \sqrt{-2\varepsilon_i}$ in which n_i is the principal quantum number of the electron orbit and ε_i is its binding energy. While this assumption $V_S(R)$ can be approximated by $V_S(R) = Z_{eff} Z_P / R$. Within the present framework, this fact that $V_S(R)$ depends only on the inter-nuclear distance gives rise to a phase factor which corresponds to the important effect of the nuclear-nuclear interaction (NN interaction) on FDCSs [19].

In this step, we withdraw the NN interaction from the total electronic Hamiltonian. Hence, H_{el} can be rearranged as [29]

$$\begin{aligned} H_{el} &= H_i + U_i + W_i = H_i^d + W_i, \\ H_{el} &= H_f + U_f + W_f = H_f^d + W_f, \end{aligned} \quad (2)$$

where H_i (H_f) is the Hamiltonian for the subsystem ($e + T$) in the entrance (exit) channel. The distortion potentials U_i and U_f are defined in such a manner that the Schrödinger equations corresponding to the distorted Hamiltonians, $H_i^d = H_i + U_i$ and $H_f^d = H_f + U_f$, are exactly solvable. Consider $\chi_i^+(\mathbf{r}, t)$ and $\chi_f^-(\mathbf{r}, t)$ as the exact solutions of the Schrödinger equations,

$$(H_i^d - i\frac{\partial}{\partial t})\chi_i^+(\mathbf{r}, t) = 0, \quad \text{and} \quad (H_f^d - i\frac{\partial}{\partial t})\chi_f^-(\mathbf{r}, t) = 0, \quad (3)$$

that satisfy the outgoing and incoming boundary conditions, respectively. Having these solutions, the perturbation potentials W_i and W_f are obtained using equations

$$\begin{aligned} (H_i - E_i)\chi_i^+(\mathbf{r}, t) &= W_i\chi_i^+(\mathbf{r}, t), \\ (H_f - E_f)\chi_f^-(\mathbf{r}, t) &= W_f\chi_f^-(\mathbf{r}, t), \end{aligned} \quad (4)$$

where E_i (E_f) is the total initial (final) energy of the system in the center-of-mass (c.m.) frame. These potentials are weaker than those appearing in the Born series, so it is expected that the distorted wave series corresponding to these perturbation potentials converge faster than those appear in Born approximation. Also, assume that $\psi_i^+(\mathbf{r}, t)$ and $\psi_f^-(\mathbf{r}, t)$ are respectively the incoming and outgoing solutions of the Schrödinger equation

$$(H_{el} - i\frac{\partial}{\partial t})\psi(\mathbf{r}, t) = 0, \quad (5)$$

with the exact asymptotic behaviors [29, 39]. The above introduced wavefunctions satisfy the conditions

$$\lim_{t \rightarrow -\infty} \langle \psi_f^- | \chi_i^+ \rangle = 0, \quad \lim_{t \rightarrow +\infty} \langle \chi_f^- | \psi_i^+ \rangle = 0, \quad (6)$$

which imply that the transition cannot be produced by the action of the distortions.

In the present version of CDW-EIS, $\chi_i^+(\mathbf{r}, t)$ and $\chi_f^-(\mathbf{r}, t)$ are approximated as [29]

$$\begin{aligned} \chi_i^+(\mathbf{r}, t) &= \Phi_i^+(\mathbf{r}, t) \mathcal{L}_i^{+EIS}(\mathbf{r}), \\ \chi_f^-(\mathbf{r}, t) &= \Phi_f^-(\mathbf{r}, t) \mathcal{L}_f^{-CDW}(\mathbf{r}), \end{aligned} \quad (7)$$

where $\Phi_i^+(\mathbf{r}, t)$ and $\Phi_f^-(\mathbf{r}, t)$ are the incoming and outgoing wavefunctions in the first Born approximation

$$\begin{aligned} \Phi_i^+(\mathbf{r}, t) &= \psi_i(\mathbf{r}_T) e^{-i(\frac{1}{2}\mathbf{v} \cdot \mathbf{r} + \frac{1}{8}\mathbf{v}^2 t + \varepsilon_i t)} \\ \Phi_f^-(\mathbf{r}, t) &= \psi_C^-(\mathbf{r}_T) e^{-i(\frac{1}{2}\mathbf{v} \cdot \mathbf{r} + \frac{1}{8}\mathbf{v}^2 t + E_f t)}, \end{aligned} \quad (8)$$

where ε_i is the initial binding energy of the electron, $\psi_i(\mathbf{r}_T)$ is the wavefunction describing its initial bound state. $\psi_C^-(\mathbf{r}_T)$ is the Coulomb distorted wavefunction describing the motion of the ejected electron in the field of the residual target ion with an explicit form of

$$\begin{aligned} \psi_C^-(\mathbf{r}_T) &= (2\pi)^{-3/2} N(\nu_T) e^{i\mathbf{k}_e \cdot \mathbf{r}_T} \\ &\times {}_1F_1(i\nu_T; 1; -ik_e r_T - i\mathbf{k}_e \cdot \mathbf{r}_T). \end{aligned} \quad (9)$$

\mathbf{k}_e is the momentum vector of the ejected electron with respect to the target ion, ${}_1F_1(a; b; z)$ is the confluent hypergeometric function and the usual normalization factor $N(\nu_T)$ is given by $N(\nu_T) = \Gamma(1 - i\nu_T)e^{-\pi\nu_T/2}$ in which $\Gamma(z)$ is Gamma function and $\nu_T = -Z_T/k_e$ is a Sommerfeld parameter.

The distortion factors of $\mathcal{L}_i^{+EIS}(\mathbf{r})$ and $\mathcal{L}_f^{-CDW}(\mathbf{r})$ are chosen so that the distorted waves, $\chi_i^+(\mathbf{r}, t)$ and $\chi_f^-(\mathbf{r}, t)$, satisfy the correct boundary conditions. The eikonal initial state distortion is a logarithmic distortion phase factor due to the Coulomb long-range remainder of the electron-projectile perturbation potential in the initial channel. From Eqs. (3) and (7), this distortion factor can be derived as $\mathcal{L}_i^{+EIS}(\mathbf{r}) = e^{-i\nu_i \ln(\nu r_P + \mathbf{v} \cdot \mathbf{r}_P)}$, where $\nu_i = Z_P/\nu$. Similarly, it can be shown that the Coulomb distortion factor representing the post-collision interaction (PCI) between the projectile ion and the active electron is a proper expression for $\mathcal{L}_f^{-CDW}(\mathbf{r})$. So, we have

$$\mathcal{L}_f^{-CDW}(\mathbf{r}) = N(\nu_P) {}_1F_1(i\nu_P; 1; -ik_P r_P - i\mathbf{k}_P \cdot \mathbf{r}_P), \quad (10)$$

where $\nu_P = -Z_P/k_P$, and $\mathbf{k}_P = \mathbf{k}_e - \mathbf{v}$ is the momentum of the ejected electron with respect to the projectile nucleus.

The perturbation potential corresponding to the above forms of the distorted waves and the distortion factors are given by [29]

$$W_i = \frac{1}{2} \nabla_{r_P}^2 + \nabla_{r_P} \cdot \nabla_{r_T}, \quad \text{and} \quad W_f = \nabla_{r_P} \cdot \nabla_{r_T}, \quad (11)$$

which are consistent with Eq. (4).

The post and prior versions of the ionization probability amplitude, described from a reference frame fixed on the target nucleus, can be respectively written as [29]

$$\begin{aligned} a_{fi}^+(\boldsymbol{\rho}) &= -i \int_{-\infty}^{+\infty} dt \langle \chi_f^- | W_f^\dagger | \psi_i^+ \rangle \\ &\simeq -i \int_{-\infty}^{+\infty} dt \langle \chi_f^- | W_f^\dagger | \chi_i^+ \rangle, \\ a_{fi}^-(\boldsymbol{\rho}) &= -i \int_{-\infty}^{+\infty} dt \langle \psi_f^- | W_i | \chi_i^+ \rangle \\ &\simeq -i \int_{-\infty}^{+\infty} dt \langle \chi_f^- | W_i | \chi_i^+ \rangle. \end{aligned} \quad (12)$$

NN interaction is not included in these versions of the transition amplitude. Also, in an exact treatment, these forms of the amplitude are mathematically equivalent, while in an approximate treatment a post-prior discrepancy may be expected.

Now, we are ready to take into account the influence of the NN interaction on the probability amplitude. Using the procedure outlined in Refs. [27, 42], this influence can be considered by multiplying the above amplitudes by a phase factor due to the pure Coulomb interaction between P and T . Accordingly, the transition amplitude including the NN-interaction influence reads

$$\mathcal{A}_{fi}^\pm(\boldsymbol{\rho}) = i(\rho\nu)^{2i\nu} a_{fi}^\pm(\boldsymbol{\rho}), \quad (13)$$

where $\nu = Z_P Z_T/\nu$ is a Sommerfeld parameter, and Z_T is the asymptotic charge of the target ion T .

Using the two-dimensional Fourier transforms, the corresponding probability amplitudes in the momentum-space can be obtained as [19, 42]

$$\begin{aligned} t_{fi}^\pm(\boldsymbol{\eta}) &= \frac{1}{2\pi} \int d\rho e^{i\boldsymbol{\eta} \cdot \boldsymbol{\rho}} a_{fi}^\pm(\boldsymbol{\rho}), \\ \mathcal{T}_{fi}^\pm(\boldsymbol{\eta}) &= \frac{1}{2\pi} \int d\rho e^{i\boldsymbol{\eta} \cdot \boldsymbol{\rho}} \mathcal{A}_{fi}^\pm(\boldsymbol{\rho}), \end{aligned} \quad (14)$$

in which $\boldsymbol{\eta}$ is the transverse momentum transfer. Inserting the inverse Fourier transform of $t_{fi}^\pm(\boldsymbol{\eta})$ into (13) and getting the Fourier transform of the result leads to

$$\mathcal{T}_{fi}^\pm(\boldsymbol{\eta}) = \frac{i\nu^{2i\nu}}{(2\pi)^2} \int d\boldsymbol{\eta}' t_{fi}^\pm(\boldsymbol{\eta}') \int d\rho \rho^{2i\nu} e^{i(\boldsymbol{\eta} - \boldsymbol{\eta}') \cdot \boldsymbol{\rho}}. \quad (15)$$

The integral over $\boldsymbol{\rho}$ can be analytically performed to obtain [19]

$$\mathcal{T}_{fi}^\pm(\boldsymbol{\eta}) = \frac{\nu}{2(2\pi)^3} \int d\boldsymbol{\eta}' t_{fi}^\pm(\boldsymbol{\eta}') |\boldsymbol{\eta} - \boldsymbol{\eta}'|^{-2(1+i\nu)}, \quad (16)$$

in which the overall phase factor of $i(\nu^2/2\pi)^{i\nu}$ is dropped since it affects neither the probability nor the cross section of the reaction. The integral over $\boldsymbol{\eta}'$ can be performed numerically to obtain the triple differential cross section for ionization of the active electron.

The fully differential cross section (FDCS) for the considered breakup process is given as [43]

$$\frac{d^5\sigma}{d^2\boldsymbol{\eta} d^3\mathbf{k}_e} = \frac{1}{4\pi^2\nu} |\mathcal{T}_{fi}(\boldsymbol{\eta})|^2 \quad (17)$$

in which $\mathcal{T}_{fi}(\boldsymbol{\eta})$ is the corresponding post or prior transition matrix element. Since $d^2\boldsymbol{\eta} d^3\mathbf{k}_e$ can be expressed in terms of the triple differential $dE_k d\Omega_e \Omega_P$, this cross section is more commonly referred to as triply differential cross sections (TDCS) for ejection of the electron with energy between E_e and $E_e + dE_e$ into solid angle $d\Omega_e$ in direction of \mathbf{k}_e and scattering of the projectile into solid angle $d\Omega_P$ in direction of \mathbf{K}_f [44].

At the end, let us refer to the main differences between the present distortion method and its fully quantum mechanical version which is known as 3DW-EIS in the literature. First, in the present model a classical straight trajectory is assumed for the projectile while such an assumption is not allowed in quantum mechanics. Second, we have used analytical wavefunctions for the initial bound and the final continuum states of the active electron, while the numerical HF wavefunctions are used for both in 3DW-EIS. Third, in 3DW-EIS amplitude there exists an extra term coming from a proper rearrangement of the terms included in the exact amplitude, and taking into account the additional higher-order effects through the final-state perturbation, while this term is absent in CDW-EIS.

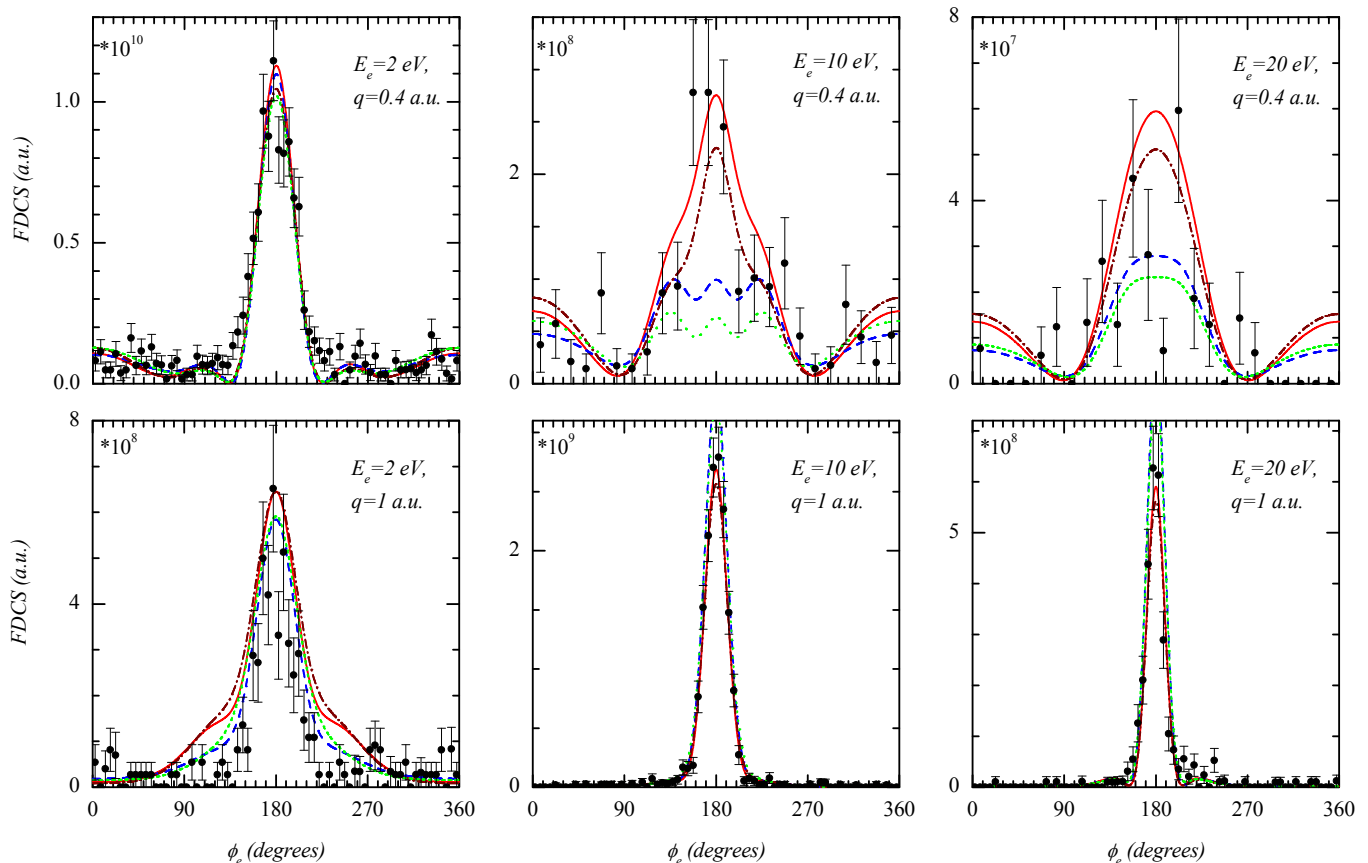


FIG. 1. (Color online) CDW-EIS FDCSs for ionization of the ground state lithium atoms are compared with their experimental values [23]. The solid (red) curves are for prior CDW-EIS with NN interaction, the dashed (blue) lines are the same but for post CDW-EIS. The dash-dotted (brown) curves are for prior calculations without NN interaction and the dotted (green) lines are the same for post calculations. Closed symbols are for experiments [24].

III. RESULTS

In this section, we use the above outlined method to study the 16 MeV Li^{2+} -impact differential single ionization of the ground ($2s$) and the first excited ($2p$) states of Li targets. To this end, the FDCSs are calculated as a function of the ejected electron's azimuthal angle for ejection into the plane perpendicular to the incident projectile beam. The results are compared with the experimental data as well as the results obtained using the fully quantum mechanical version of the theory (or 3DW-EIS theory), which both have been recently reported in Ref. [24]. We choose the origin of the coordinate system at the target nucleus T , with the z -axis along the incident beam. It is assumed that the projectile is scattered in the $+xz$ half plane and the positive direction of the y axis is chosen so it makes a right-handed coordinate system. The azimuthal and polar angles of the ejected electron is measured as usual with respect to the positive directions of the x and z axes, respectively.

In addition to the ionization occurring in the Li^{2+} - Li collisional system, some other processes like electron

capture by Li^{2+} , excitation or ionization of the inner shell electrons in the target atom and even the ionization of the projectile ion may occur during the collision process. However, since our considered experimental data are for the outer shell ionization of the target, we neglected the other possible reactions.

For three different values of the ejected-electron's energy, $E_e = 2, 10,$ and 20 eV, and two different values of the projectile momentum transfer, $q = |\mathbf{K}_i - \mathbf{K}_f| = 0.4,$ and 1 a.u., the calculated post and prior FDCSs for single ionization of lithium atoms in their ground states are compared with their experimental values in figure 1. Both post and prior cross sections with and without NN interaction are included in this figure. In order to do a meaningful comparison, in each case the prior results with the NN interaction are normalized to the experiment at the binary peak, and the other results are multiplied by the same normalization factor. Considering the figure, several points are remarkable: as is kinematically expected, in accordance with the experiments, the theory predicts a binary peak at $\phi_e = 180^\circ$. For cases ($E_e = 2$ eV, $q = 0.4$ a.u.), ($E_e = 10$ eV, $q = 1$ a.u.),

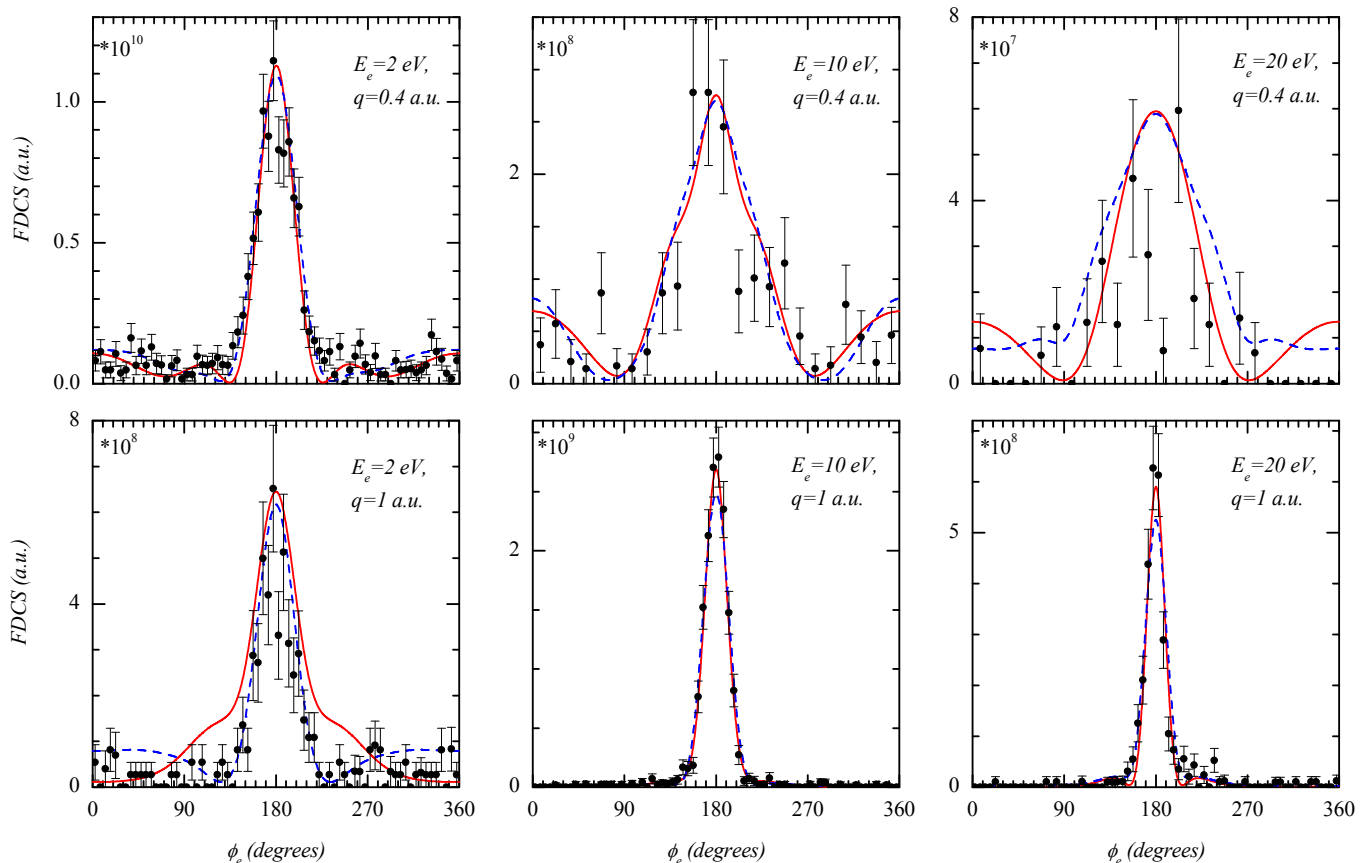


FIG. 2. (Color online) Comparison of the full prior CDW-EIS cross sections with their corresponding values obtained using the 3DW-EIS model and with the measured data. Solid (red) curves are for CDW-EIS, dashed (blue) curves for 3DW-EIS and closed symbols for experiments.

and ($E_e = 20$ eV, $q = 1$ a.u.), the NN interaction has no considerable influence on the cross sections and the post-prior discrepancy is very small. However, for these cases, maximum of the both of these effects occurs at the binary peak. For ($E_e = 2$ eV, $q = 1$ a.u.), the post-prior discrepancy is observed both at $\phi_e = 180^\circ$ and at two mirror-symmetric angular regions on both sides of the binary peak. In this case, the NN interaction plays a minor role. For $E_e = 10$ and 20 eV cases with $q = 0.4$ a.u., both the post-prior discrepancy and the NN-interaction influence are quite obvious. This means that for higher emission energies and lower momentum transfers, the influence of both the NN interaction and the post-prior discrepancy on the cross sections is considerable. This effect becomes much more important around the binary peak for which a structure is seen in the results. For the cases ($E_e = 10$ eV, $q = 1$ a.u.) and ($E_e = 20$ eV, $q = 1$ a.u.) around the binary peak, the prior values are upper than the post results, while the situation is reversed for the same energies but the lower momentum transfers. It is interesting that the shape of the post and prior results is nearly the same in all cases, except for ($E_e = 10$ eV, $q = 1$ a.u.) and ($E_e = 20$ eV, $q = 1$ a.u.).

Although, on the whole, good overall agreement is found between the calculations and the experimental data in all cases, it seems the prior calculations with considering the NN interaction gives a better description of the collision dynamics. It is probable that the results would be improved both in shape and in magnitude by considering the procedure outlined in Refs. [36] and/or [38].

It should be also remarked that in order to keep the present model in a three-body framework, the projectile is assumed as a bare ion. Although the obtained results show that this assumption is not too far from reality, the influence of the projectile-electron on the cross sections can be examined using a more complicated four-body model. For the cases that agreement of the calculations with experiments is poor, such an approach probably improves the results, but it is not followed here.

FDCSs for ionization of $Li(2s)$ targets calculated using the prior version of CDW-EIS including the NN interaction are compared with their corresponding results obtained using the 3DW-EIS model [24] and with their experimental values [24] in figure 2. The results of both theories are normalized to the experiments at the binary peak. As is seen from this figure, it is interesting that in

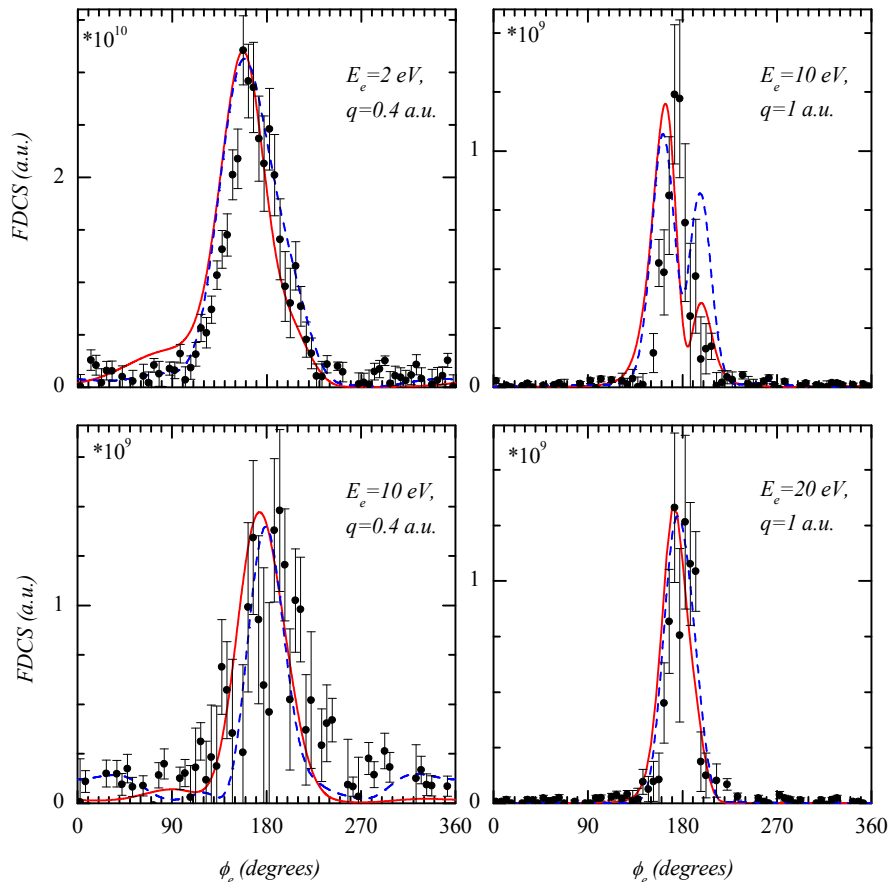


FIG. 3. (Color online) Same as figure 2 but for ionization of $Li(2p)$ targets.

the cases for which the influence of the NN-interaction and post-prior discrepancy on the cross sections is insignificant, the theories completely coincide with each other at all the azimuthal angles. In these cases, both theories are also in good accordance with experiments. The most difference between the semiclassical CDW-EIS and the full quantum 3DW-EIS theories occurs for lower ejection energies but higher momentum transfers such as ($E_e = 2$ eV, $q = 1$ a.u.) and for higher energies but lower momentum transfers such as ($E_e = 20$ eV, $q = 0.4$ a.u.). For these cases, it seems that 3DW-EIS is in better agreement with the measured data.

A similar comparison is made for single ionization of the $2p$ excited states of Li targets in figure 3. Since the targets were experimentally prepared [24] with relative populations of 86%, 9%, and 5% for the magnetic substates with $m = -1$, $m = 0$, and $m = 1$, respectively, the cross sections are calculated using these experimental weights. If the sublevels with $m = \pm 1$ were equally populated, a symmetric angular distribution is expected for both the calculated and the measured cross sections around $\phi_e = 180^\circ$. But for this case, since these two substates are not equally populated, this distribution is asymmetric. This behavior which is known as magnetic

dichroism (or orientational dichroism) in the angular distribution of the electron emission is exhibited in figure 3.

Like the case of the $2s$ state, the post-prior discrepancy is also seen for ionization of the $2p$ -excited state, but it is much smaller than that was found in figure 1 for the ground $2s$ state. Also, for all the specified cases represented in figure 2, the influence of the NN interaction on the cross sections is unimportant. Consequently, the post and prior CDW-EIS cross sections with and without NN interaction are nearly the same. For this fact, only the prior CDW-EIS including the NN interaction (the full prior CDW-EIS) results are illustrated in the figure.

In most of the case studies of the typical ion-atom collisional reactions, it has been shown that the inter-nuclear interaction plays a major role in the differential cross sections, while the role changes to a minor contribution, or not influence at all, in the integrated cross sections. Here, at least for most of the present considered cases, the comparisons show that the role of the inter-nuclear interaction is not crucial even in the fully differential cross sections.

Interestingly, the theory predicts a double peak structure for ($E_e = 10$ eV, $q = 1$ a.u.) around $\phi_e = 180^\circ$. The second peak predicted by 3DW-EIS is higher than that is

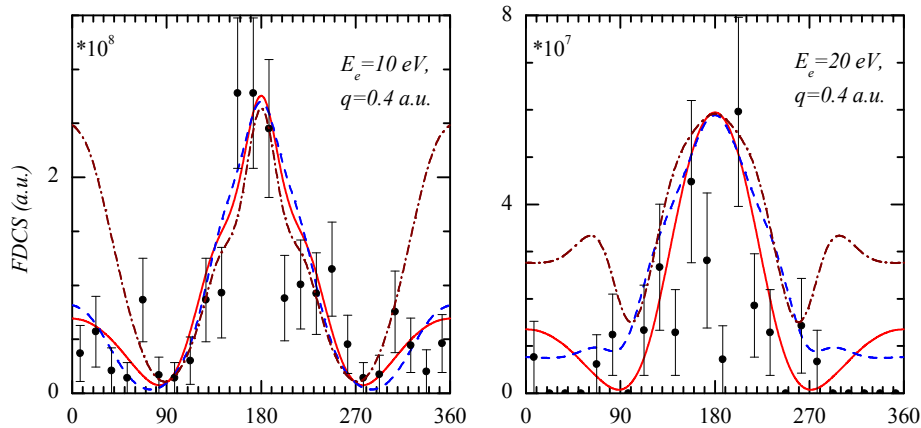


FIG. 4. (Color online) Comparison of experimental and theoretical 3DW-EIS, CDW-EIS and FBA FDCS results for 16 MeV Li^{2+} ionization of the $2s$ shell of Li in the azimuthal plane as a function of the azimuthal angle. Symbols are for experiments, solid (red) curves for the prior CDW-EIS, dashed (blue) curves for 3DW-EIS, and dash-dotted (brown) curves for FBA.

predicted by CDW-EIS. Although double-peak structure seems to be real, it is not seen vividly in the measured cross sections probably for the low resolution of the experiments. However, to further confirm the reality of this theoretically predicted behavior further experiments with better resolution should be carried out. It should be noted even if the predicted structure be real, the binary peak in the left part of the panel is slightly more shifted to left than experimental data. The present calculations confirm this hypothesis that the predicted double-peak structure is attributed to the angular distribution of the initial bound-state wavefunction of the ejected electron and the kinematics only. However, the general kinematical conditions under which occurrence of such a structure is predictable are still questionable. For ($E_e = 10$ eV, $q = 0.4$ a.u.) the peak position shifts slightly to left with respect to the 3DW-EIS predictions and the measured data.

It may be asserted that the reasonable agreement of the obtained results with experiment is not surprising, since even the first Born approximation (FBA) is expected to be reasonable at sufficiently high impact energies. In order to examine the validity of such a hypothesis, we compared the $2s$ -ionization results for ($E_e=10$ eV, $q = 0.4$ a.u.) and ($E_e=20$ eV, $q = 0.4$ a.u.) with the FBA approximation in figure 4. As is seen, at the angular regions far from the binary peak, the agreement of FBA with experiments is very poor, while the CDW-EIS and 3DW-EIS results are in reasonable agreement with the measurements in these angular regions.

Comparison of the theoretical predictions for ionization of $Li(2p)$ in the cases ($E_e = 2$ eV, $q = 1$ a.u.) and ($E_e = 20$ eV, $q = 0.5$ a.u.) is instructive, although there do not exist available experimental cross sections for these cases. This comparison is performed in figure 5. The full post and prior CDW-EIS cross sections and the 3DW-EIS results are depicted in this figure. For both cases, the NN interaction does not considerably change

the cross sections neither in shape nor in magnitude, while the post-prior discrepancy is completely obvious in some angular regions. However most of the aspects in the post and prior graphs are the same.

For these cases, the 3DW-EIS [24] and CDW-EIS theories predict totally different behaviors for the ejected electron spectra. Such an obvious difference has been also reported between 3DW-EIS and FBA [24]. For ($E_e = 2$ eV, $q = 1$ a.u.), CDW-EIS predicts a double binary peak structure, while the 3DW-EIS predicts a single right-shifted binary peak. Also, the width of the peak structures is very different in both predictions. Such a double peak structure is predicted by both theories for ($E_e = 10$ eV, $q = 1$ a.u.). According to the 3DW-EIS predictions for that case, the lower peak goes from left to right passing through the classically expected peak position when the projectile momentum transfer is kept constant at $q = 1$ a.u. but E_e increases gradually from 4 eV to 16 eV [24]. We examined this point using the CDW-EIS theory, and found that the double peak structure appears even for emission energies lower than 1 eV. Interestingly, such a similar situation was observed when we kept q at 1.2 a.u. and changed E_e in the same range. Also, for higher values of q , such a double peak structure is observable at various energy intervals. For example, two peaks with nearly the same heights is observed for $q = 1.2, 1.5$ and 2 a.u. at $E_e = 8, 18$ and 40 eV, respectively. This means that in the CDW-EIS and 3DW-EIS theories the kinematical conditions under which the double peak structure appears are different. So, further experimental studies are necessary to identify the correct conditions.

For ($E_e = 20$ eV, $q = 0.5$ a.u.), this double-peak structure disappears, instead, two nearly mirror-symmetric shoulders appears in both sides of the binary peak in the 3DW-EIS cross sections. In the post and prior CDW-EIS results these shoulders are of course absent and only a relatively sharp peak is seen. Also, both theories pre-

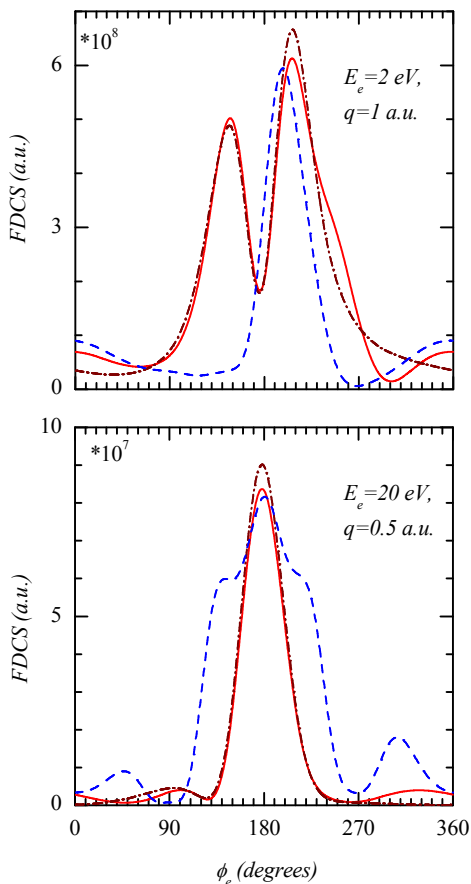


FIG. 5. (Color online) Comparison of the full post and prior CDW-EIS calculations with the 3DW-EIS results. Solid (red) curves are for the prior CDW-EIS, dash-dotted (brown) curves for the prior CDW-EIS and dashed (blue) curves for 3DW-EIS.

dict some structures in angular domains of $[0^\circ, 90^\circ]$ and $[270^\circ, 360^\circ]$ in both side of the peak region. Post-prior discrepancy is relatively large in these angular regions and also at the binary peak angle. Also for this case, the results of the 3DW-EIS and CDW-EIS theories are obviously different and since there is no experimental data in hand, we cannot conclude which one of the theoretical methods can explain the mechanism in these cases better.

It may be discussed that since the 3DW-EIS and CDW-EIS do not employ the same electronic states, it is difficult to judge whether the extra term of the quantum transition amplitude or the different approximations for the electronic states is the main source of the differences observed in the calculations in some cases. In order to clarify this point, we recall that the 3DW-EIS results are not so sensitive to the radial part of the wavefunctions [24]. Since the angular part of the employed wavefunctions are the same in both theories, so the difference of the electronic wavefunctions cannot be the source of the discrepancies observed between the 3DW-EIS and

CDW-EIS results. However, it is worthy to point out that, in some cases, using the same numerical HF wavefunctions employed in 3DW-EIS, the CDW-EIS theory produces the results in very good accordance with the quantum considerations [35, 37, 41]. For example, a semi-classical CDW-EIS approach with numerical HF wavefunctions [41] is recently used to simulate a recent precise experiment [45] and a very good agreement with the experiment was found.

It may be argued that with the study based on the fully quantum-mechanical version of CDW-EIS already reported in Ref. [24], there is no room for publication of the present study with two more approximations: 1) classical straight-line motion for the projectile, 2) the employment of the hydrogenic Coulomb wave functions for the description of the target of *Li*. In order to rebut such a presumption, we would like to highlight several points as follow: i) As the reader affirms, the present model is a semi-classical model while the other one is a fully quantum-mechanical approach. So the calculations are very different but in most of the cases the results are close to each other. ii) In this contribution, we focused on the NN interaction and for some specified cases it has been shown that the NN interaction plays a minor role in the collision dynamics even the fully differential cross section is the case. iii) In this paper, we investigated the post-prior discrepancies observed in the calculated fully differential cross sections, while such a discussion is absent in Ref. [24]. We showed for some cases this discrepancy is much more important than the nuclear-nuclear interaction. iv) Here, we showed that for some cases, FBA is not a good theory, although the impact energy is high enough. v) In the present work, it has been shown that for some values of E_e and q , the predictions made by the 3DW-EIS and CDW-EIS are very different, and in Ref. [24] it has been shown that for the same cases the 3DW-EIS results are clearly different from FBA results. Consequently, there are some cases where 3DW-EIS, CDW-EIS and FBA predictions are very different. vi) Both 3DW-EIS and CDW-EIS theories predict a double binary peak structure for some cases. However, we showed that the kinematical conditions leading to such a structure are different in the theories. For the last two points, further experimental data is needed to judge the validity of the theoretical predictions.

IV. CONCLUSIONS

The three-body CDW-EIS method was used to theoretical study of the single ionization of the neutral lithium atoms in the $Li^{2+} - Li$ collision systems. Detachment of the outer electron from $Li(2s)$ and $Li(2p)$ by impact of 16 MeV Li^{2+} ions was considered. The FDCSs for ejection of the outgoing electron into the azimuthal plane were calculated as a function of the ejected electron's azimuthal angle. Both post and prior cross sections were evaluated. For different values of the ejected electron

energy (E_e) and the projectile momentum transfer (q), the obtained results were compared with the similar calculations performed using the quantum version of the formalism. This later version of the theory is labeled as 3DW-EIS in the literature to distinguish from CDW-EIS. Also, in the cases for which experimental data is available the results were compared to those data.

For ionization of $Li(2s)$, in the cases for which the binary peak is relatively sharp and it is well demystified in the measurements, the agreement of the results with the 3DW-EIS and with experiments is very good. For such cases, the NN interaction does not play a significant role in the break up process. Also, the post-prior discrepancy is small for these cases. But, for the cases that the experimental data are too diverse to clearly illustrate the binary peak, some discrepancies was found between CDW-EIS and 3DW-EIS theories. For these cases, both the role of the NN interaction in the reaction and the influence of the post-prior discrepancy on the cross sections become more obvious.

For ionization of $Li(2p)$, in the cases for which there exist experimental data, the overall agreement between CDW-EIS and experiment is reasonable. However, some small differences are observed between CDW-EIS and 3DW-EIS. For example, for ($E_e = 10$ eV, $q = 0.4$ a.u.), these differences were observed both in the shape and in the peak position predicted for the angular distribution of the cross sections by these theories. Also, for ($E_e = 10$ eV, $q = 1$ a.u.), both theories predict a double-peak structure for the cross sections, but the second peak

predicted by 3DW-EIS is much higher than that of CDW-EIS. Our calculations showed that this structure is attributed to the angular part of the initial bound state wavefunction of the active electron and to the kinematical conditions. In contrast to these differences the overall agreement of the theories seems fair. For, these cases both the NN interaction and the post-prior discrepancy play a minor role in the calculated results.

The major difference between the CDW-EIS and 3DW-EIS theories takes place for ionization of $Li(2p)$ in the cases for which there is no experiential data. For ($E_e = 2$ eV, $q = 1$ a.u.), CDW-EIS predicts a double-peak structure, while such a complex structure is absent in the 3DW-EIS predictions. Also, 3DW-EIS predicts two shoulders in both sides of the binary peak, while these shoulders are absent in the CDW-EIS results. Consequently the kinematical conditions for occurring a double-peak structure are different in these theories. Further experiments are needed to indicate which one of these sets of predictions are real. For these cases, the NN interaction is not important but the post-prior discrepancy is considerable in some angular regions and at the binary-peak angle.

ACKNOWLEDGMENTS

OG would like to acknowledge the office of graduate studies at the University of Isfahan for their support and research facilities.

-
- [1] N. Stolterfoht, R. D. DuBois, and R. D. Rivarola, *Electron Emission in Heavy Ion-Atom Collisions* (Springer, New York, 1997)
- [2] W. F. Drake, *Springer Handbook of Atomic, Molecular, and Optical Physics* (Springer, Berlin, 2006)
- [3] M. Schulz, and D. H. Madison, *Int. J. Mod. Phys. A* **21**, 3649 (2006)
- [4] M. Schulz, R. Moshhammer, D. Fischer, H. Kollmus, D. H. Madison, S. Jones, and J. Ullrich, *Nature* **422**, 48 (2003)
- [5] T. Rescigno, M. Baertschy, W. A. Isaacs, and C. E. McCurdy, *Science* **286**, 2474 (1999)
- [6] D. H. Madison, and O. Al-Hagan, *J. Atom. Mol. Opt. Phys.* **2010**, 367180 (2010)
- [7] E. Ehrhardt, M. Schulz, T. Tekaath, and K. Willmann, *Phys. Rev. Lett.* **22**, 89 (1969)
- [8] A. Lahmann-Bennani, *J. Phys. B: At. Mol. Opt. Phys.* **24**, 2401 (1991)
- [9] J. Röder, H. Ehrhardt, C. Pan, A. F. Starace, I. Bray, and D. V. Fursa, *Phys. Rev. Lett.* **79**, 1666 (1997)
- [10] A. Dorn, R. Moshhammer, C. D. Schröter, T. J. M. Zouros, W. Schmitt, H. Kollmus, R. Mann, and J. Ullrich, *Phys. Rev. Lett.* **82**, 2496 (1999)
- [11] M. A. Haynes, and B. Lohmann, *J. Phys. B: At. Mol. Opt. Phys.* **33**, 4711 (2000)
- [12] J. Ullrich, R. Moshhammer, A. Dorn, R. Dörner, L. Schmidt, and H. Schmidt-Böcking, *Rep. Prog. Phys.* **66**, 1463 (2003)
- [13] R. R. Dörner, V. Mergel, O. Jagutzki, L. Spielberger, J. Ullrich, R. Moshhammer, and H. Schmidt-Böcking, *Phys. Rep.* **330**, 192 (2000)
- [14] D. Fischer, D. Globig, J. Goullon, M. Grieser, R. Hubele, V. L. B. de Jesus, A. Kelkar, A. LaForge, H. Lindenblatt, D. Misra, B. Najjari, K. Schneider, M. Schulz, M. Sell, and X. Wang, *Phys. Rev. Lett.* **109**, 113202 (2012)
- [15] R. Hubele, M. Schuricke, J. Goullon, H. Lindenblatt, N. Ferreira, A. Laforge, E. Brühl, V. L. B. de Jesus, D. Globig, A. Kelkar, D. Misra, K. Schneider, M. Schulz, M. Sell, Z. Song, X. Wang, S. Zhang, and D. Fischer, *Rev. Sci. Instrum.* **86**, 033105 (2015)
- [16] J. Colgan, and M. S. Pindzola, *Eur. Phys. J. D* **66**, 284 (2012)
- [17] R. E. Olson and J. Fiol, *Phys. Rev. Lett.* **95**, 263203 (2005)
- [18] L. Sarkadi, *Phys. Rev. A* **82**, 052710 (2010)
- [19] M. F. Ciappina, W. R. Cravero, *J. Phys. B: At. Mol. Opt. Phys.* **39**, 2183 (2006)
- [20] L. Gulyas, S. Egri, T. Kirchner, *Phys. Rev. A* **90**, 062710 (2014)
- [21] H. R. J. Walters, and C. T. Whelan, *Phys. Rev. A* **85**, 062701 (2012)
- [22] H. R. J. Walters, and C. T. Whelan, *Phys. Rev. A* **92**, 062712 (2015)

- [23] E. Ghanbari-Adivi, D. Fischer, N. Ferreira, J. Goullon, R. Hubele, A. LaForge, M. Schulz, and D. Madison, *Phys. Rev. A* **94**, 022715 (2016)
- [24] E. Ghanbari-Adivi, D. Fischer, N. Ferreira, J. Goullon, R. Hubele, A. LaForge, M. Schulz, and D. Madison, *J. Phys. B: At. Mol. Opt. Phys.* **50**, 215202 (2017)
- [25] E. Clementi, and C. Roetti, *At. Data Nucl. Data Tables* **14**, 177 (1974)
- [26] D. S. F. Crothers, *J. Phys. B: At. Mol. Opt. Phys.* **15**, 2061 (1982)
- [27] D. S. F. Crothers, and J. F. McCann, *J. Phys. B: At. Mol. Opt. Phys.* **16**, 3229 (1983)
- [28] A. Salin, *J. Phys. B: At. Mol. Opt. Phys.* **22** 3901 (1989)
- [29] P. D. Fainstein, V. H. Ponce, and R. D. Rivarola, *J. Phys. B: At. Mol. Opt. Phys.* **24** 3091 (1991)
- [30] H. F. Busnengo, A. Martínez, R. D. and Rivarola, *J. Phys. B: At. Mol. Opt. Phys.* **29**, 4193 (1996)
- [31] V. D. Rodríguez, and R. O. Barrachina, *Phys. Rev. A* **57** 215 (1998)
- [32] L. Gulyás, and P. D. Fainstein, *J. Phys. B: At. Mol. Opt. Phys.* **31**, 3297 (1998)
- [33] J. Fiol, and V. D. Rodríguez, and R. O. Barrachina, *J. Phys. B: At. Mol. Opt. Phys.* **34**, 933 (2001)
- [34] A. B. Voitkiv, B. Najjari, and J. Ullrich, *J. Phys. B: At. Mol. Opt. Phys.* **36**, 2591 (2003)
- [35] A. B. Voitkiv, and B. Najjari, *J. Phys. B: At. Mol. Opt. Phys.* **37**, 4831 (2004)
- [36] P. N. Abufager, P. D. Fainstein, A. E. Martínez, and R. D. Rivarola, *J. Phys. B: At. Mol. Opt. Phys.* **38**, 11 (2005)
- [37] A. B. Voitkiv, and B. Najjari, *Phys. Rev. A* **79**, 022709 (2009)
- [38] J. M. Monti, O. A. Fojón, J. Hanssen, and R. D. Rivarola, *J. Phys. B: At. Mol. Opt. Phys.* **43**, 205203 (2010)
- [39] Dz. Belkić, I. Mancev, J. Hanssen, *Rev. Mod. Phys.* **80**, 249 (2008)
- [40] M. F. Ciappina, C. A. Tachino, R. D. Rivarola, S. Sharma, and M. Schulz, *J. Phys. B: At. Mol. Opt. Phys.* **48**, 115204 (2015)
- [41] A. B. Voitkiv, *Phys. Rev. A* **95**, 032708 (2017)
- [42] D. P. Dewangan, and J. Eichler, *Phys. Rep.* **247**, 59 (1994)
- [43] A. B. Voitkiv, and J. Ullrich, *Phys. Rev. A* **67**, 062703 (2003)
- [44] D. Fischer, R. Moshhammer, M. Schulz, A. Voitkiv, and J. Ullrich, *J. Phys. B: At. Mol. Opt. Phys.* **36**, 3555 (2003)
- [45] H. Gassert, O. Chuluunbaatar, M. Waitz, F. Trinter, H.-K. Kim, T. Bauer, A. Laucke, Ch. Müller, J. Voigtsberger, M. Weller, J. Rist, M. Pitzer, S. Zeller, T. Jahnke, L. Ph. H. Schmidt, J. B. Williams, S. A. Zaytsev, A. A. Bulychev, K. A. Kouzakov, H. Schmidt-Böcking, R. Dörner, Yu. V. Popov, and M. S. Schöffler, *Phys. Rev. Lett.* **116**, 073201 (2016)